Received: 16 June 2020 | Revised: 9 November 2020 | Accepted: 14 December 2020

DOI: 10.1002/asl.1023

RESEARCH ARTICLE

Atmospheric Science Letters RMetS

Rossby wave packets in the upper troposphere and their associations with climatological summertime daily precipitation in MLRYR of China

Siyuan Sun | **Zhaoyong Guan**

Collaborative Innovation Center on Forecast and Evaluation of Meteorological Disasters (CIC-FEMD), Key Laboratory of Meteorological Disaster, Ministry of Education (KLME), International Joint Laboratory on Climate and Environment Change (ILCEC), Nanjing University of Information Science and Technology, Nanjing, China

Correspondence
Zhaoyong Guan, Nanjing University of Information Science and Technology, No.219, Ningliu Rd., Nanjing 210044, China.
Email: guanzy@nuist.edu.cn

Funding information
National Key R&D Program of China, Grant/Award Number: 2019YFC1510201; China Meteorological Administration Special Public Welfare Research Fund, Grant/Award Number: GYHY201406024

[Correction added on 8 January 2021, after first online publication. The sequence of Funding information has been updated in this version.]

Abstract

Using the NCEP/NCAR reanalysis and station observations in China during 1979–2018, features of propagation of baroclinic wave packets in the upper troposphere and their relationships with precipitation over the middle and lower reaches of the Yangtze River (MLRYR) in daily climatology are investigated after having components with periods longer than 9 days filtered out. It is demonstrated that in the filtered daily climatology, the baroclinic wave packets still exist. The wave packet migrates eastward on the northern sides of the westerly jet stream axis whereas it does not move explicitly in the southern side of the axis in the upper troposphere. The filtered daily precipitation over MLRYR is mainly affected by the wave packets in the region south of the westerly jet axis. These results are very meaningful for better understanding behaviors of Rossby waves in daily climatology and the causes of daily precipitation variations in MLRYR.

KEYWORDS

boreal summer, China, daily climatology, precipitation, wave packet

1 | INTRODUCTION

The region of the middle and lower reaches of the Yangtze River (MLRYR), located in eastern China, has abundant precipitation in the summer due to the influence of the East Asian summer monsoon (Lu *et al*., 2002; Guan and Yamagata, 2003). Precipitation in MLRYR varies largely not only in spatial but also in temporal on interannual and decadal scales (Zhang *et al*., 2007; Ma *et al*., 2012). During some years, heavy rainstorms frequently occur in this region, leading to severe floods there. These rainstorm events are usually induced by synoptic and mesoscale systems in this region (Wang *et al*., 2016; Li *et al*., 2016a).

Precipitation in MLRYR is affected by various internal atmospheric dynamical processes and external forcings (Kuang and Zhang, 2006). Baroclinic Rossby waves embedded in the mid-latitude westerlies (Huang *et al*., 2014; O'Brien and Reeder, 2017; Wei *et al*., 2017) are associated with weather and climate in the mid-latitude (Hoskins and Ambrizzi, 1993; Chang, 1999; Enomoto *et al*., 2003; Tan, 2008; Hong *et al*., 2018), including precipitation extremes (Ryoo *et al*., 2013; Tozer *et al*., 2018). Under certain conditions, Rossby waves can form wave packets that

propagate from upstream to downstream in the westerlies, directly influencing weather and climate in MLRYR and Huai River Basins. In years when higher than normal precipitation occurs in these basins, Rossby wave packet activity is always obviously observed in the upper troposphere in the mid-latitude, whereas very weak wave packets are observed in years with much less rainfall (Mei and Guan, 2008, 2009). On the interannual and decadal time scales, Rossby waves also have pronounced influences on MLRYR although the Rossby wave energy dispersion demonstrates different features on these time scales (Li *et al*., 2016b).

Previous studies have indicated that precipitation in MLRYR is closely related to wave packet activities in the upper troposphere (Shi *et al*., 2009; Ye *et al*., 2019a); each individual precipitation event is affected by the wave packet activities (Li *et al*., 2018; Ye *et al*., 2019a, 2019b). All the above studies (e.g., Mei and Guan, 2008, 2009; Ye *et al*., 2019a, 2019b) suggest that the wave packets are observed in the upper troposphere in particular years. However, in reality, a time-varying quantity can be separated into the multi-year mean climatology and the departures from this mean climatology. It is reported that the migratory baroclinic Rossby wave as well as its wave packets are robustly found in the anomalous daily circulations (e.g., Chang, 1999; Mei and Guan, 2008, 2009). Then some questions rise as are the migratory wave packets still found in multi-year averaged daily data? The answers to these questions are very important for us to understand the behavior of Rossby waves. More than this, it is also necessary to clarify if there are any relationships between these wave packets and the variation of multi-year averaged daily precipitation. Therefore, the purpose of the present work is to investigate the wave packet activities in the upper troposphere in daily climatology with examining the possible relations with daily precipitation in MLRYR. The results of the present study will be helpful for in-depth understanding of daily climate in the Yangtze River basin and the mechanism behind.

2 | DATA AND METHOD

The data used in the present study include (a) daily winds and geopotential height at all 12 pressure levels provided from the earth surface up to 100 hPa, which are extracted from global 2.5° × 2.5° NCEP/NCAR reanalysis product (Kalnay *et al*., 1996), and (b) daily precipitation collected at 2425 weather stations in China in the summer during 1979–2018, which are extracted from Dataset of Basic Meteorological Elements at National Weather Stations in China. Summer refers to June–July in the Northern Hemisphere. Note that June–July is the focus period in the present article because it is the months when Meiyu/Baiu occurs during this period of time.

The daily climatology is obtained by averaging the June–July daily data over 40 years from 1979 to 2018. In daily climatology, the seasonal cycle is most dominant. To examine the high-frequency component, perturbation in the present paper is defined as variations with periods shorter than 10 days, which is obtained from 40-year mean daily climatology by using a Lanczos filter (Duchon, 1979). The effective degree of freedom is estimated when the statistical test is performed for regression.

Wavenumbers between 5 and 7 are usually dominant in the meridional wind perturbations at 300 hPa in the upper troposphere (Kao and Wendell, 1970; Mei and Guan, 2008, 2009) although they are different in different years (Ye *et al*., 2019b). However, the dominant zonal wavenumbers of 40-year mean filtered daily meridional wind averaged over (30–60°N) at 300 hPa are found to be 7–9 in the present study. After the dominant wavenumbers are fixed, the wave packets are then obtained. The Hilbert transform can effectively extract baroclinic wave packets from the meridional wind perturbation field (Zimin *et al*., 2003). The envelope of wave packet can be expressed as: $Ve = abs\left(v' + i*\hat{v'}\right)$, where v' is the meridional wind perturbation at 300 hPa, $\hat{v'}$ is the Hilbert transform of v', and Ve is the envelope parameter.

The Rossby wave dispersion relative to the mean flow is also partly explored using the wave activity fluxes (WAF) proposed by Takaya and Nakamura (2001). The wave activity flux is expressed as

$$\mathbf{W} = \mathbf{C}_{\mathrm{U}} M + \mathbf{W}_{\mathrm{r}},$$

$$\mathbf{W}_{\mathrm{r}} = \frac{p}{2|\mathbf{U}|}\begin{bmatrix} U\left(\psi'^{2}_{x} - \psi'\psi'_{xx}\right) + V\left(\psi'_{x}\psi'_{y} - \psi'\psi'_{xy}\right) \\ U\left(\psi'_{x}\psi'_{y} - \psi'\psi'_{xy}\right) + V\left(\psi'^{2}_{y} - \psi'\psi'_{yy}\right) \end{bmatrix},$$

where $\mathbf{W}$ is the WAF, $\mathbf{C}_{\mathrm{U}}$ the phase speed of the Rossby wave along the basic flow, M the pseudo-momentum of wave activity, and $\mathbf{W}_{\mathrm{r}}$ the WAF relative to effects of basic flow (WAFr hereafter). Both M and $\mathbf{W}_{\mathrm{r}}$ are derived from quasi-geostrophic stream-function departure ψ' and other meteorological variables (Li *et al*., 2016a). In the westerlies, the Rossby waves that determine the weather usually move eastward to downstream. If the phase speed is smaller enough, the $\mathbf{W}_{\mathrm{r}}$ will approximately exhibit the propagation directions of the Rossby wave energy (e.g., Ke and Guan, 2014).

3 | CLIMATOLOGICAL FEATURES OF SUMMER PRECIPITATION AND MID-LATITUDE CIRCULATION

The 40-year average of summer precipitation (shaded in Figure 1a) in eastern China shows a "more in the south—less in the north" pattern with the large

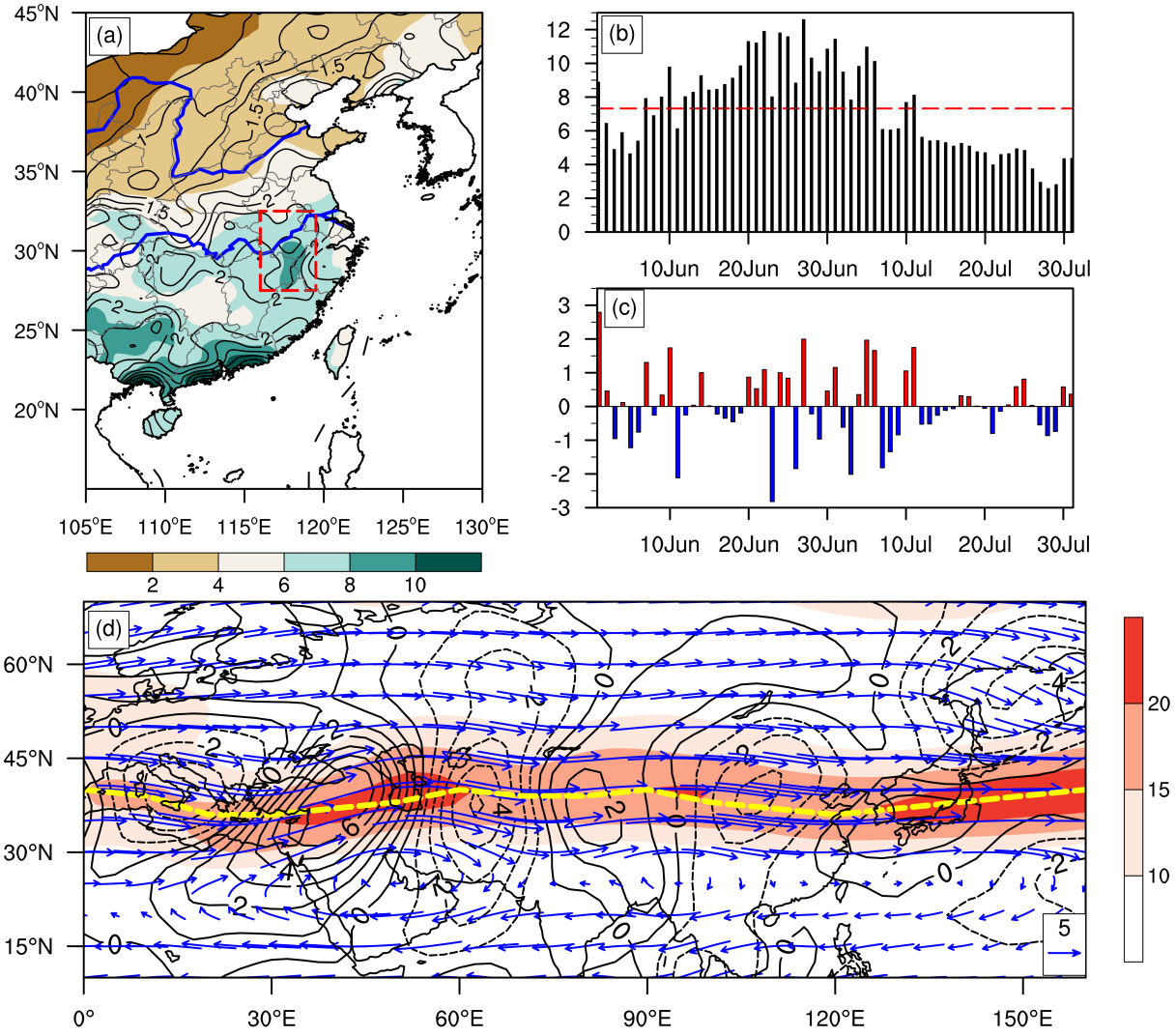

FIGURE 1 The 40-year mean daily climatology of summer (June–July) precipitation (shaded, mm/d) in eastern China and the standard deviations (contours, mm/d) of daily precipitation after variation components with periods longer than 9 days have been filtered out (a), the time series of 40-year mean daily precipitation (bars, mm/d) along with its summertime mean (red dashed horizontal line) averaged over (27.5–32.5°N, 116–119.5°E) in MLRYR (b), the time-series of precipitation after components with periods longer than 9 days filtered out (c), and 40-year mean climatology of summer circulation at 300 hPa (d) with reddish shades (black contours, solid for positive while dashed for negative values) for zonal (meridional) wind component, blue arrows for winds (m/s), the thick yellow dashed line for the westerly jet-stream axis at 300 hPa. Two thick blue lines in (a) are respectively for the Yangtze River in southern and Yellow River in northern parts of China

precipitation located in the middle and lower reaches of and to the south of the Yangtze River. After having variation components with periods longer than 9 days removed out, the climatological daily precipitation exhibits its larger standard deviations (black contours in Figure 1a) in the region (27.5–32.5°N, 116–119.5°E) (Box-A, hereafter). Time series of daily precipitation averaged over Box-A is presented in Figure 1b, which is computed using the continuous and reliable observations collected at 109 weather stations, indicating that daily precipitation is largely concentrated over the period from middle June to early July with a large variation in the daily total amount. After having data preprocessed using a high-pass filter, it indicates that the daily variations in precipitation (Figure 1c) still exist clearly with maximum difference about 6 mm/d between positive and negative values in 40-year mean summertime daily climatology. We will focus on these high-frequency variations (1–9 day component) in both precipitation and circulations in the present study.

The westerly jet stream in the upper troposphere above Asia extends zonally with the axis locate at around 40°N (Figure 1d). Large westerly wind speeds are found near the Caspian Sea, the Black Sea, and the Mediterranean Sea, corresponding to the entrance of the jet streak; similarly, another area of large westerly wind speeds is located near 90°E and the Japan Sea, corresponding to

the exit of the jet streak. The mid-latitude westerly jet in the upper troposphere as a whole is continuous and strong, which is favorable for the formation of waveguides and downstream propagation of waves (Ambrizzi and Hoskins, 1997). The distribution of mean climatological meridional wind (Figure 1d) shows that there exists a waveguide with its axis along 40°N.

The baroclinic waves are clearly observed in 40-year mean daily climatology after variation components with periods longer than 9 days have been filtered out. It is seen from Figure 2a that a cyclonic circulation at 850 hPa is found to be just over Box-A in MLRYR when more precipitation occurs there. But at 300 hPa, the significant southwest winds are observed over Box-A (Figure 2b), indicating the baroclinic structure in vertical over MLRYR (Figure 2a). This kind of baroclinic disturbance is migratory. It is seen from Figure 2c that the meridional wind perturbation (v') propagates eastward along the climatological jet stream, with a phase speed of about 600 km/d. However, the wave energy propagation of these disturbances in the filtered meridional wind is not so clearly observed in Figure 2c along this jet-stream. It may be clearly explored by examining the WAF. Additionally, it can be seen from Figure 2c that the major period of meridional disturbances near 120°E is found to be about 6 days, which is consistent with results reported by Blackmon (1976), Orlanski and Chang (1993), and Wirth *et al.* (2018) who pointed out that baroclinic eddies are transient features with a typical period of about 5–10 days.

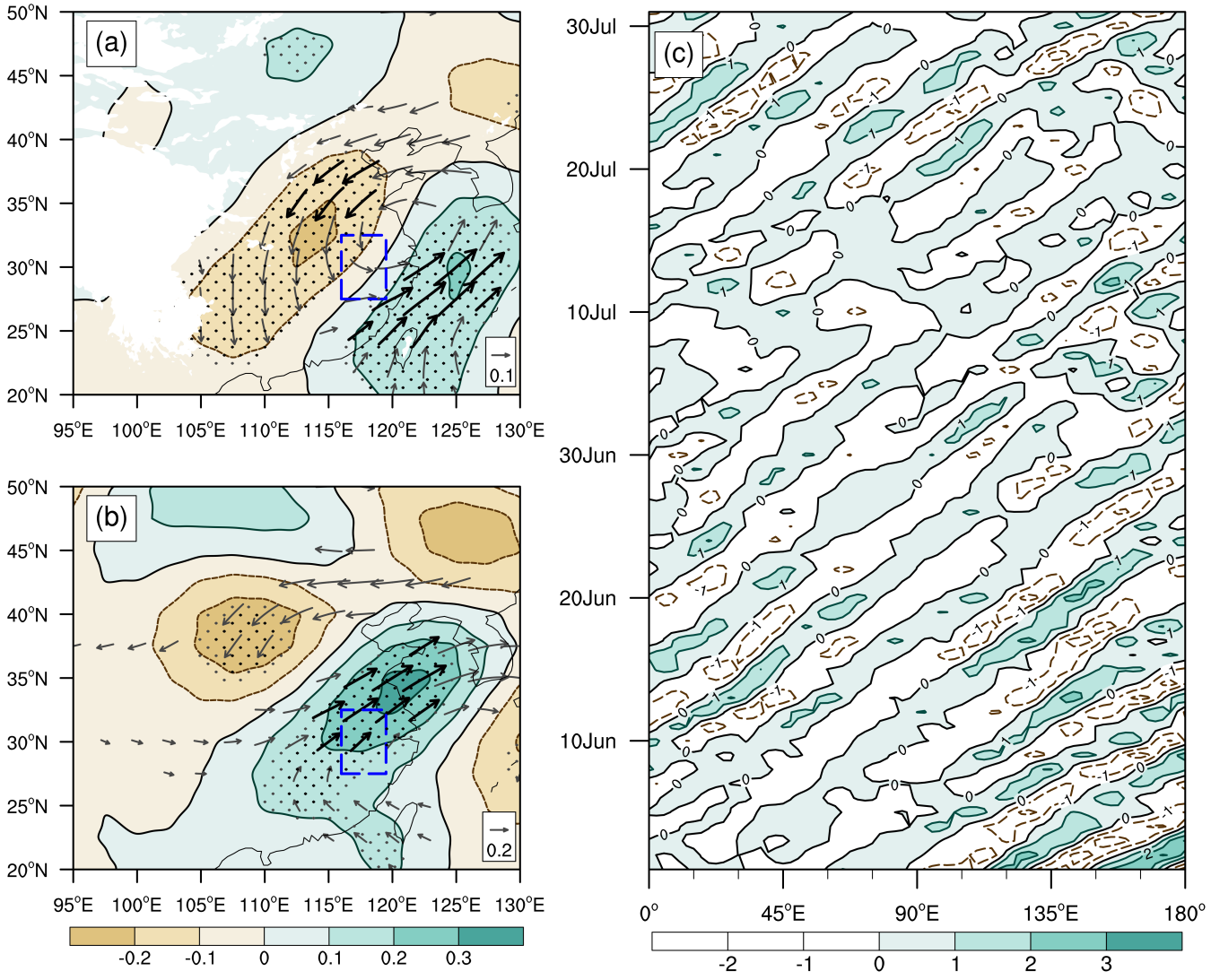

FIGURE 2 Regressed winds (arrows) along with their meridional components (shaded) at 850 hPa (a) and 300 hPa (b) as obtained by regressing the filtered summer daily winds onto the time-series of filtered rainfall averaged over Box-A in MLRYR. Arrows displayed in black (gray) are those with both (either) the zonal (u') and (or) meridional (v') wind components at/above 95% confidence level. Shades are for the regressed v' with stipples in black (gray) for values at/above 95% (90%) confidence level. The effective degree of freedom is found to be about 48. Shown in (c) is the time-longitude cross-section of filtered daily climatological meridional wind v' (in m/s) at 300 hPa averaged over (32.5–45°N) in boreal summer

4 | WAVE PACKETS IN FILTERED CLIMATOLOGICAL DAILY WINDS

In order to analyze the wave energy propagation, the range of wavenumbers must be identified first (Chang, 1999). It is found that wavenumbers of the dominant baroclinic waves in the upper troposphere in the mid-latitude are typically 5–7 (Chang and Yu, 1999; Mei and Guan, 2009) but they are different in different years (Ye *et al.*, 2019b). However, in the filtered meridional wind of 40-year mean summer daily climatology, waves with wavenumbers 7–9 are found to be dominant in latitude belt from 30°N to 60°N. This indicates that the daily changes still exist in filtered multi-year mean summer daily climatology although some cancelations of high-frequency perturbations when 40-year mean are calculated. By performing the Hilbert transform (Zimin *et al.*, 2003) of the filtered time-series of meridional

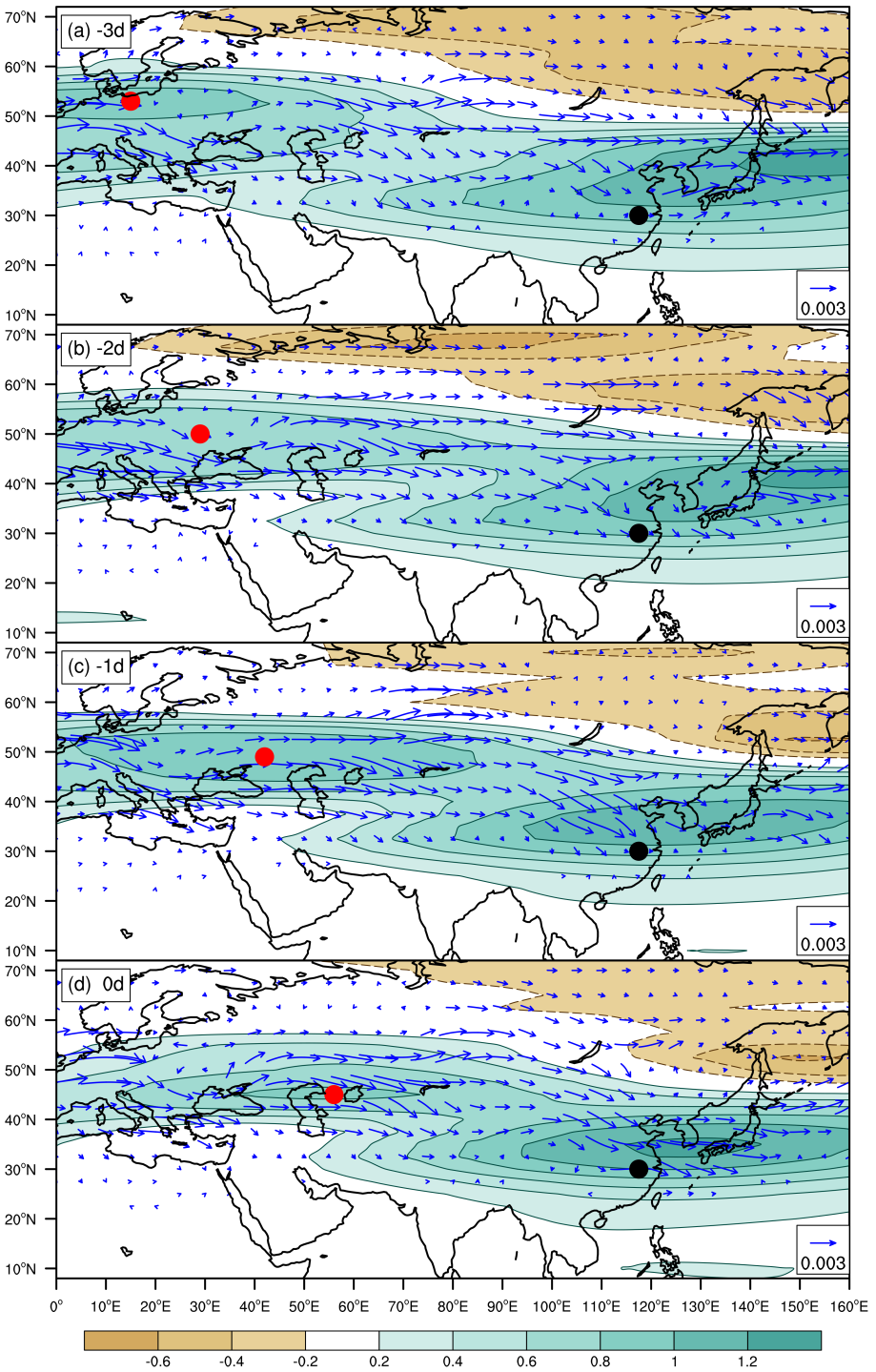

FIGURE 3 One-point time-lag regressions (greenish shaded contours) as obtained by regressing *Ve*, which is derived from filtered time-series of 40-year mean summer in the study domain, onto *Ve* at base point (black thick dot). Big red dots are for the center of wave packet in the region west of 60°E. Arrows in blue are for the wave activity fluxes $\mathbf{W}_r$, which are derived from the geostrophic stream function by employing the regressions analysis considering the time-lags. The time lags are set to be −3d to 0d (a-d). The base point is located at (30°N, 117.5°E), the intervals for both shades and contours are 0.2

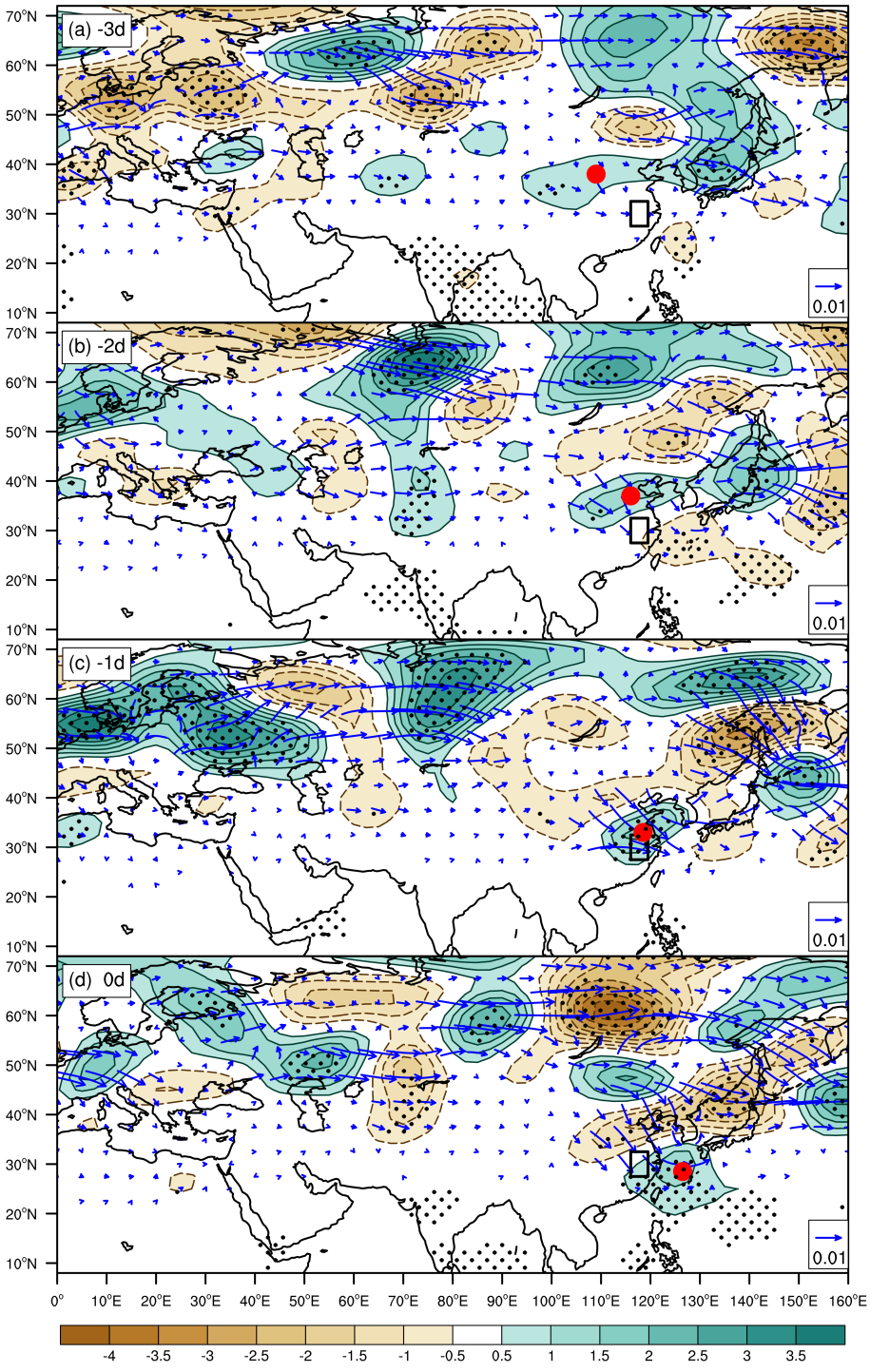

FIGURE 4 Time-lag regressions (shaded contours) as obtained by regressing the 300 hPa geopotential height which is derived from filtered time-series of 40-year mean summer in the study domain onto filtered time-series of precipitation $P_r^{'}$ averaged over Box-A. Big red dots are for indicating the movement of the disturbance centers near MLRYR. Arrows in blue are for the wave activity fluxes $\mathbf{W}_r$, which are derived from the regressed geopotential height by employing the regression analysis considering the time-lags with precipitation $P_r^{'}$. The time lags are set to be from −3d to 0d (a-d), respectively. The black rectangular frame is for Box-A. The contour intervals are 0.5 with greenish shades for positive and brownish for negative values. Stippled with black color are for anomalous geopotential height at/above 90% level of confidence

winds, the envelope parameter *Ve* for the wave packet is then obtained.

The propagation features of baroclinic Rossby wave packets at 300 hPa related to summer *Ve* variations in MLRYR can be observed in the time-lagged one-point regressions (Figure 3). The one-point regression is defined as the regressions between *Ve* in the study domain and *Ve* at the base point (30°N, 117.5°E) corresponding to the center of the maximum standard deviation of filtered summer precipitation in 40-year mean daily climatology (Figure 1a).

The wave packet in daily climatology for processes with periods shorter than 10 days exhibits a zonally stretched structure. Figure 3 shows that there are two strong *Ve* zones (greenish shaded contours); the one is located south of 40°N from about 55°E to the region beyond the eastern board of the study domain (southern wave packet) whereas the other north of this latitude

from the Prime Meridian eastward to about 85°E (northern wave packet). This phenomenon suggests that, climatologically, the Rossby wave packets in transient disturbances tend to propagate in the zones north or south of the jet stream axis, which is very different from results reported by Ambrizzi and Hoskins (1997) who shows the westerly jet stream act westerlies as a waveguide for quasi-stationary Rossby waves in a numerical simulation. The formation of the double zones for wave packets of synoptic-scale waves needs to be clarified. It may be due to the jet-stream structure as a waveguide for different kinds of waves with different wavelengths and different speeds, and hence suggesting that the jet-stream axis may act as a border to wave energy propagations of the migrating waves.

The wave packet in the region north of jet stream axis migrates southeastward quickly from −3d to 0d whereas it does not in the region south of the jet stream axis (Figure 3a-d). It works out that the zonal speed of the northern wave packet migration as denoted by red thick dots in Figure 3 is about 11.0°lon./day. But, the phase speed of high-frequency Rossby waves as seen in Figure 2c is apparently large, being estimated at about 6.5°lon./day in mid-latitude at 300 hPa. This indicates that the phase speed of waves is much slower than that of the wave energy dispersion for the northern wave packet.

The southern wave packet denoted by *Ve* elongating from 55°E eastward to Pacific in the southern flank of Asian Jet stream axis does not look to move in zonal (Figure 3a-d). This looks quite different from the northern wave packet. Theoretically, for waves with zonal wavelength larger than the meridional wavelength, the zonal component of group velocity may be zero in a slow varying basic flow (Hoskins *et al*., 1983). Of course, except for the wave packet intensity gets a little stronger from −3d to 0d (Figure 3a-d), the behaviors of the wave packets in the filtered 40-year mean summer daily climatology look quite different from those in some particular years (Ye *et al*., 2019a), especially years such as 1998 and 2003 when the severe flood events occurred in MLRYR (Mei and Guan, 2008, 2009; Ye *et al*., 2019b). In those years, the wave packets at 300 hPa migrate very quickly from regions near the Caspian Sea eastward/southeastward to East China.

The wave activity fluxes $\mathbf{W}_r$ (WAFrs) exhibit the eastward propagation of Rossby wave energy, being consistent with eastward migration of the wave packet. It can be clearly seen from Figure 3 that the WAFrs start from the region north of the Mediterranean Sea and propagate eastward to MLRYR. The southern and the northern wave packets can be linked with each other in the region around (40°N, 80°E) by the wave energy propagation as denoted by WAFrs. Some bigger arrows are found in the zonal direction between the northern and the southern wave packet although there are WAFrs differences between region near Europe and East Asia (Figure 3) along the jet streak (Figure 1d). From Figure 3a-d, it is seen that both the WAFrs and the southern wave packet look relatively weaker on −3d to −1d when the time series of the entire field leads the series at the base point than those on 0d. In other words, although the southern wave packet center does not move much, the WAF looks intensifying in MLRYR (around thick black dots in Figure 3), which is consistent with the strengthening of the southern wave packet over MLRYR.

To further examine the wave behaviors in association with precipitation variations in MLRYR, the disturbances of geopotential height at 300 hPa and related WAFrs are presented in Figure 4, which is obtained from the geopotential height regressed upon the filtered time-series of precipitation. It is seen from Figure 4 the waves move eastward very quickly in mid-latitude Europe. Simultaneously, the WAFrs exhibit the wave energy dispersing eastward in zonal, which is in agreement with the northern wave packet migrations.

However, the moving direction of the disturbance in eastern part of China looks clearly different from that in mid-latitude Europe; it clearly moves southeastward, especially in meridional (Figure 4a-d). In the zonal direction, the disturbances are always stronger in East China along latitudes such as 30°N. This can partly explain why the southern wave packet keeps stationary in zonal. It is seen from Figure 4 that, during the period from −3d to 0d, the perturbation center of the geopotential height in the region east of 110°E moves southeastward from 40°N to about 30°N; the speed of the perturbation center migration is roughly estimated as 3.3°lat./d. The WAFrs display that there is relatively strong propagation of Rossby wave energy from the region near (40°N, 110°E) (Figure 4a) to MLRYR (Figure 4d), further suggesting the precipitation variations in MLRYR are influenced by baroclinic wave packet in the upper troposphere.

5 | CONCLUSION

In 40-year mean daily precipitation climatology, apparently changes are still observed in eastern China during boreal summer, especially in the middle and lower reaches of Yangtze River (MLRYR). In some years, heavy precipitation in MLRYR is highly correlated with activities of Rossby wave packets embedded in the mid-latitude westerly belt (Mei and Guan, 2008, 2009). In the present study, it is found that signals of Rossby wave packets displayed by *Ve* can still be detected in 1–9 day band-pass

filtered 40-year mean climatological daily fields although the waves with zonal wavenumbers 7–9 rather than usually 5–7 are dominant in meridional wind departures.

Two Rossby wave packets are respectively found in zones on the north and south sides of the westerly jet stream axis. The wave packets move at different group velocities in different zones. The northern wave packet migrates eastward very quickly, whereas the southern one almost does not move in the zonal direction. There are wave energy propagations from the northern to the southern wave packet. The MLRYR precipitation variations are influenced by these two wave packets, especially by the southern one as well as its related circulation variations over MLRYR.

Note that daily climate variability in MLRYR is under the influence of wave packet activities embedded in the mid-latitude westerlies. However, the dominant zonal wave number is found to be 7–9 in daily climatology after the high-filtering is performed, which is quite different from 5 to 7 in particular years. This may be partly due to the cancelation of disturbances in multi-year mean. The wave activity fluxes converge into MLRYR, possibly inducing the wave energy to increase or remain the same there (Figures 3 and 4). Moreover, the precipitation appears to be more influenced by the wave packets in the zone south of the westerly jet stream axis (Figure 3). Besides, as Rossby waves are extremely important in precipitation in MLRYR, the Rossby wave breaking (e.g., Ndarana and Waugh, 2011) may also play a role in influencing circulation variations over MLRYR. Why are these phenomena induced? What makes these? These questions deserve further studies in the near future.

ACKNOWLEDGEMENTS

This work is jointly supported by the National Key Research and Development Program of China (2019YFC1510201), the China Meteorological Administration Special Public Welfare Research Fund (GYHY201406024), and PAPD project of Jiangsu Province. Precipitation data are from the archives in National Meteorological Information Center. The NCEP/NCAR reanalysis products are provided by NOAA CIRES Climate Diagnostics Center (http://www.cdc.noaa.gov). All figures in the paper are produced using NCL (NCAR Command Language).

ORCID

Siyuan Sun https://orcid.org/0000-0001-6391-8220

REFERENCES

Ambrizzi, T. and Hoskins, B.J. (1997) Stationary Rossby-wave propagation in a baroclinic atmosphere. *Quarterly Journal of the Royal Meteorological Society*, 123(540), 919–928.

Blackmon, M.L. (1976) A climatological spectral study of the 500 mb geopotential height of the northern hemisphere. *Journal of the Atmospheric Sciences*, 33(8), 1607–1623.

Chang, E.K.M. (1999) Characteristics of wave packets in the upper troposphere. Part II: seasonal and hemisphere variations. *Journal of the Atmospheric Sciences*, 56(11), 1729–1747.

Chang, E.K.M. and Yu, D.B. (1999) Characteristics of wave packets in the upper troposphere. Part I: Northern hemisphere winter. *Journal of the Atmospheric Sciences*, 56(11), 1708–1728.

Duchon, C.E. (1979) Lanczos filtering in one and two dimensions. *Journal of Applied Meteorology*, 18(8), 1016–1022.

Enomoto, T., Hoskins, B.J. and Matsuda, Y. (2003) The formation mechanism of the Bonin high in August. *Quarterly Journal of the Royal Meteorological Society*, 129(587), 157–178.

Guan, Z.Y. and Yamagata, T. (2003) The unusual summer of 1994 in East Asia: IOD teleconnections. *Geophysical Research Letters*, 30(10), 1544. https://doi.org/10.1029/2002GL016831.

Hong, X.W., Lu, R.Y. and Li, S.L. (2018) Asymmetric relationship between the meridional displacement of the Asian westerly jet and the silk road pattern. *Advances in Atmospheric Sciences*, 35 (4), 389–396.

Hoskins, B.J. and Ambrizzi, T. (1993) Rossby wave propagation on a realistic longitudinally varying flow. *Journal of the Atmospheric Sciences*, 50(12), 1661–1671.

Hoskins, B.J., Ian, N.J. and White, G.H. (1983) The shape, propagation and mean-flow interaction of large-scale weather systems. *Journal of the Atmospheric Sciences*, 40(7), 1595–1612.

Huang, D.Q., Zhu, J., Zhang, Y.C. and Huang, A.N. (2014) The different configurations of the east Asian polar front jet and subtropical jet and the associated rainfall anomalies over eastern China in summer. *Journal of Climate*, 27(21), 8205–8220.

Kalnay, E., Kanamitsu, M., Kistler, R., Collins, W., Deaven, D., Gandin, L., Iredell, M., Saha, S., White, G., Woollen, J., Zhu, Y., Leetmaa, A., Reynolds, R., Chelliah, M., Ebisuzaki, W., Higgins, W., Janowiak, J., Mo, K.C., Ropelewski, C., Wang, J., Jenne, R. and Joseph, D. (1996) The NCEP/NCAR 40-year reanalysis project. *Bulletin of the American Meteorological Society*, 77(3), 437–471.

Kao, S.K. and Wendell, L.L. (1970) The kinetic energy of the large-scale atmospheric motion in wavenumber-frequency space I: northern hemisphere. *Journal of the Atmospheric Sciences*, 27 (3), 359–375.

Ke, D. and Guan, Z.Y. (2014) Variations in regional mean daily precipitation extremes and related circulation anomalies over central China during boreal summer. *Journal of Meteorological Research*, 28(4), 524–539.

Kuang, X.Y. and Zhang, Y.C. (2006) Impact of the position abnormalities of East Asian subtropical westerly jet on summer precipitation in middle-lower reaches of Yangtze River. *Plateau Meteorology*, 25(3), 382–389 (in Chinese).

Li, M.G., Guan, Z.Y., Jin, D.C., Han, J. and Zhang, Q. (2016a) Anomalous circulation patterns in association with two types of daily precipitation extremes over southeastern China during boreal summer. *Journal of Meteorological Research*, 30(2), 183–202.

Li, M.G., Guan, Z.Y. and Mei, S.L. (2016b) Interannual and interdecadal variations of summer rainfall duration over the middle and lower reaches of the Yangtze River in association with anomalous circulation and Rossby wave activities. *Chinese Journal of Atmospheric Sciences*, 40(6), 1199–1214 (in Chinese).

Li, X., Guan, Z.Y. and Ye, D.C. (2018) Characteristics of Rossby wave packets in non-ENSO years and their possible impacts on severe precipitation events in the middle and lower reaches of Yangtze River in summer: a glimpse in 1993. *Transactions of Atmospheric Sciences*, 41(2), 167–175 (in Chinese).

Lu, R.Y., OH, J.H. and Kim, B.J. (2002) A teleconnection pattern in upper-level meridional wind over the North African and Eurasian continent in summer. *Tellus A*, 54(1), 44–55.

Ma, Y., Chen, W., Fong, S., Leong, K. and Leong, W. (2012) Interannual and interdecadal variations of precipitation over eastern China during Meiyu season and their relationships with the atmospheric circulation and SST. *Chinese Journal of Atmospheric Sciences*, 36(2), 397–410 (in Chinese).

Mei, S.L. and Guan, Z.Y. (2008) Activities of baroclinic wave packets in the upper troposphere related to Meiyu of 2003 in the Yangtze River-Huaihe River valley. *Chinese Journal of Atmospheric Sciences*, 32(6), 1333–1340 (in Chinese).

Mei, S.L. and Guan, Z.Y. (2009) Propagation of baroclinic wave packets in upper troposphere during the Meiyu period of 1998 over middle and lower reaches of Yangtze River valley. *Journal of Tropical Meteorology*, 25(3), 300–306 (in Chinese).

Ndarana, T. and Waugh, D.W. (2011) A climatology of Rossby wave breaking on the southern hemisphere tropopause. *Journal of the Atmospheric Sciences*, 68(4), 798–811.

O'Brien, L. and Reeder, M.J. (2017) Southern hemisphere summertime Rossby waves and weather in the Australian region. *Quarterly Journal of the Royal Meteorological Society*, 143(707), 2374–2388.

Orlanski, I. and Chang, E.K.M. (1993) Ageostrophic geopotential fluxes in downstream and upstream development of baroclinic waves. *Journal of the Atmospheric Sciences*, 50(2), 212–225.

Ryoo, J.M., Kaspi, Y., Waugh, D.W., Kiladis, G.N., Waliser, D.E., Fetzer, E.J. and Kim, J. (2013) Impact of Rossby wave breaking on U.S. west coast winter precipitation during ENSO events. *Journal of Climate*, 26(17), 6360–6382.

Shi, N., Bueh, C., Ji, L.R. and Wang, P.X. (2009) The impact of mid- and high-latitude Rossby wave activities on the medium-range evolution of the EAP pattern during the pre-rainy period of South China. *Acta Meteorologica Sinica*, 23(3), 300–314.

Takaya, K. and Nakamura, H. (2001) A formulation of a phase-independent wave-activity flux for stationary and migratory quasi-geostrophic eddies on a zonally varying basic flow. *Journal of the Atmospheric Sciences*, 58, 608–627.

Tan, B.K. (2008) Advances of atmospheric of Rossby waves dynamics. *Acta Meteorologica Sinica*, 66(6), 870–879 (in Chinese).

Tozer, C.R., Risbey, J.S., O'Kane, T.J., Monselesan, D.P. and Pook, M.J. (2018) The relationship between wave trains in the southern hemisphere storm track and rainfall extremes over Tasmania. *Monthly Weather Review*, 146(12), 4201–4230.

Wang, L., Qian, Y., Zhang, Y.C., Zhao, C., Leung, L.R., Huang, A. and Xiao, C.L. (2016) Observed variability of summer precipitation pattern and extreme events in East China associated with variations of the east Asian summer monsoon. *International Journal of Climatology*, 36(8), 2942–2957.

Wei, W., Zhang, R.H., Wen, M. and Yang, S. (2017) Relationship between the Asian westerly jet stream and summer rainfall over central Asia and North China: roles of the Indian monsoon and the South Asian high. *Journal of Climate*, 30(2), 537–552.

Wirth, V., Riemer, M., Chang, E.K.M. and Martius, O. (2018) Rossby wave packets on the midlatitude waveguide—a review. *Monthly Weather Review*, 146(7), 1965–2001.

Ye, D.C., Guan, Z.Y. and Jin, D.C. (2019a) Climatic features of summertime baroclinic wave packets over Eurasia and the associated possible impacts on precipitation in southern China. *Atmospheric Science Letters*, 20(4), e889. https://doi.org/10.1002/asl.889.

Ye, D.C., Guan, Z.Y., Sun, S.Y., Li, X. and Xia, Y. (2019b) The relationship between heavy precipitation in the middle and lower reaches of Yangtze River and baroclinic wave packets in the upper troposphere during the Meiyu period of 2016. *Acta Meteorologica Sinica*, 77(1), 73–83 (in Chinese).

Zhang, Q.Y., Lv, J.M., Yang, L.M., Wei, J. and Peng, J.B. (2007) The interdecadal variation of precipitation pattern over China during summer and its relationship with the atmospheric internal dynamic processes and extra-forcing factors. *Chinese Journal of Atmospheric Sciences*, 31(6), 1290–1300 (in Chinese).

Zimin, A.V., Szunyogh, I., Patil, D.J., Hunt, B.R. and Ott, E. (2003) Extracting envelopes of Rossby wave packets. *Monthly Weather Review*, 131, 1011–1017.

How to cite this article: Sun S, Guan Z. Rossby wave packets in the upper troposphere and their associations with climatological summertime daily precipitation in MLRYR of China. *Atmos Sci Lett*. 2021;22:e1023. https://doi.org/10.1002/asl.1023